

Stephen D. Burk and T. Haack  
Naval Research Laboratory  
Monterey, California

## 1. Introduction

Sharp vertical gradients within atmospheric thermodynamic profiles in the boundary layer (BL) can create abrupt changes in the refractivity field, thereby impacting the propagation of electromagnetic (EM) waves. This study uses the Naval Research Laboratory's Coupled Ocean/Atmosphere Mesoscale Prediction System (COAMPS<sup>TM</sup>) to investigate refractive structure (particularly at radio and microwave frequencies) during the period (April-May 2000) of a field experiment at Wallops Island, VA. Measurements taken by groups from DOD laboratories, universities, and elsewhere included low-elevation radar frequency pathloss, meteorological conditions (e.g., from buoys, rocketsondes, helicopter profiles), and radar clutter returns (an extensive description of the field campaign appears in TR-01/132 of the Naval Surface Weapons Division, Dahlgren Division).

The "Delmarva" or Tidewater Peninsula along which Wallops Island lies (the Chesapeake Bay to the west and the Atlantic Ocean to the east) contains complex topographic and land surface characteristics, as well as pronounced spatial SST variability, all contributing to complex BL structures (e.g., internal BL's; sea/land breezes; coastal jets). To explore the COAMPS fidelity in forecasting subtle BL and refractivity variations in this region, initially we nest COAMPS down to an inner grid mesh having 3 km spacing (with plans to go to 1 km) and utilize high vertical resolution in the first several hundred meters above the surface.

During the field experiment, measurements were collected along radials extending SE from the coast at Wallops I. a distance of ~65 km over the Atlantic. Similarity theory permits computation of evaporation duct height (EDH) based on the standard meteorological and oceanographic

measurements taken during Wallops 2000. Model forecast EDH values may then be compared with those computed from observations. The nature of the refractivity profile above the surface layer (e.g., subrefractive, standard, superrefractive, trapping) was measured by the rocketsondes and helicopter profiles, including horizontal variations in refractive conditions along the measurement path. The ability of COAMPS to predict the correct refractive structure and its variation along the measurement path will be assessed.

Given the difficulty of this forecasting task, model shortcomings are anticipated and will be quantified; the data set will be used to explore and test methods of improving model parameterizations, boundary conditions, etc. Upon completion of such mesoscale model refinements, propagation forecasts using model refractivity fields will be compared with measured propagation factors and model fields will be used as background for refractivity inversion techniques (e.g., refractivity from clutter, RFC; Rogers 1997)).

## 2. Modeling Aspects

The COAMPS mesoscale model used in the present study is described in Hodur et al. (2002). The model is nonhydrostatic and uses multiple nests having different horizontal resolution. It features a full suite of physical parameterizations, including a level 2.5 turbulence parameterization, radiation, and cloud microphysics schemes. Surface fluxes and surface stress are computed from the Louis scheme. Data assimilation is accomplished using a multivariate optimal interpolation (MVOI) approach.

The COAMPS model simulation for this study utilizes the grid structure shown in Fig 1 (not including 1km grid yet).

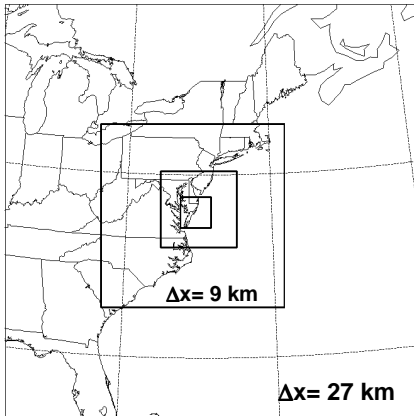


Fig. 1 (a) COAMPS nested grid structure in this study.

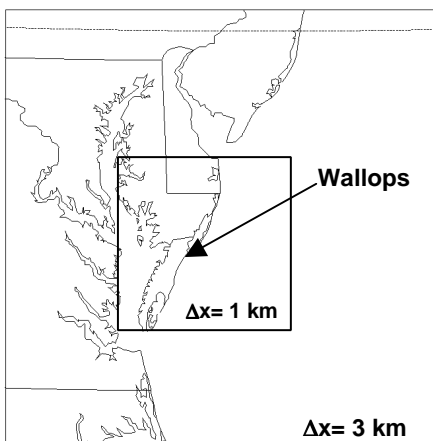


Fig. 1(b) COAMPS innermost grid meshes.

Forty vertical levels are used for the model forecasts. Because our interest in this study is particularly with very shallow, subtle features of the coastal refractivity profile, we strongly compress the model grid points near the surface. In the lowest 105 m the vertical grid spacing is 5, 15, 25, 35, 45, 55, 67.5, 85, and 105 m.

We have conducted several recent studies of refractivity in coastal regions and near islands using COAMPS (Haack and Burk 2001; Burk *et al.* 2003).

### 3. Preliminary Results

The first time period of the Wallop-2000 field experiment that we address with the COAMPS™ model is 10-12 April 2000 (days 101-103). The surface synoptic maps for 12 UTC 10 Apr show a 992 mb low over the Gulf of St. Lawrence; a 1028 mb high offshore of South Carolina; and an E-W

oriented cold front crossing WVA, VA and lying just south of Wallops Island. At 500 mb the trough lies somewhat west of the surface low over the Gulf of St. Lawrence and strong, zonal flow exits across the Tidewater Peninsula. By 12 UTC on 11 Apr., the 500 mb flow over Wallops I. has weakened and front has become stationary very close to Wallops. On 12 UTC 12 Apr. a 1016 mb surface low is now centered near the Bay of Fundy with a long cold front extending SW across the Wallops region. The high-pressure center over the Atlantic has moved eastward. Thus, this is a very challenging time period to forecast synoptic conditions (much less mesoscale/boundary layer features) in the Wallops I. region because a front is positioned in the vicinity—sometimes slightly north, sometimes slightly south—virtually the entire 3-day period. Consistent with this picture, the Naval PostGraduate School flux buoy shows numerous reversals of wind direction (southerly <-> northerly) during this period.

Figure 2a shows the 24h forecast COAMPS 10-m winds (vectors; shading) and surface pressure (mb) isobars valid 00 UTC 11 Apr 2000 (on the outermost grid). At this time, the Tidewater region is under the influence of southerly surface flow associated with the western branch of the high situated off of the Carolinas. However, as noted above, there clearly is a frontal zone in the very near proximity.

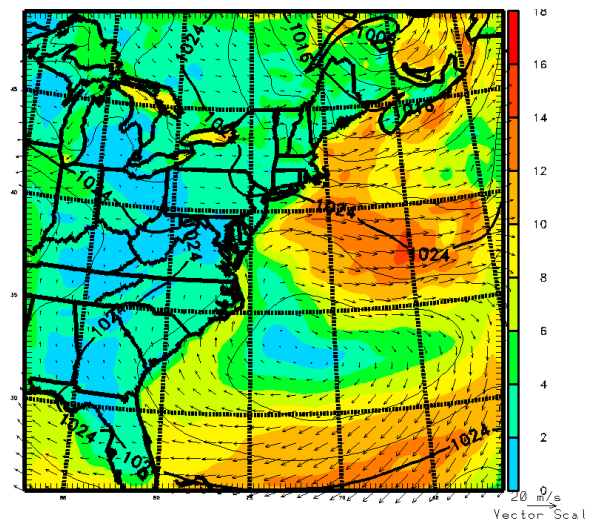


Fig. 2(a) COAMPS 10m wind forecast.

Displayed in Fig. 2b is the forecast on the 3 km grid of 10-m wind vectors, shaded sea

surface temperature (K), and surface pressure at the same time as Fig. 2b.

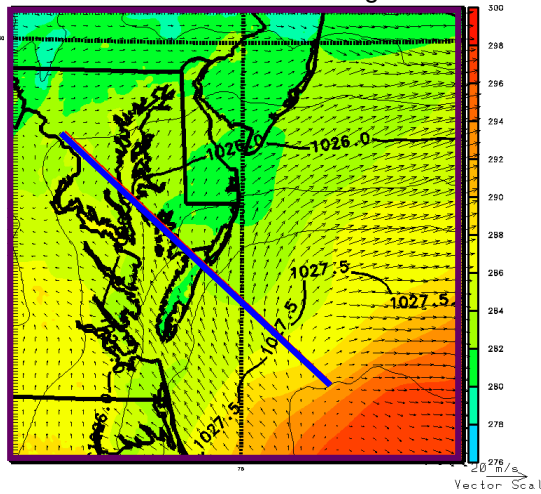


Fig. 2b COAMPS 3 km grid forecast.

The SST warms considerably from the coast to the SE corner of this grid, with more subtle SST variations in the immediate vicinity of the coast. Figure 2b also shows a line along which a vertical cross section is displayed in Fig. 3.

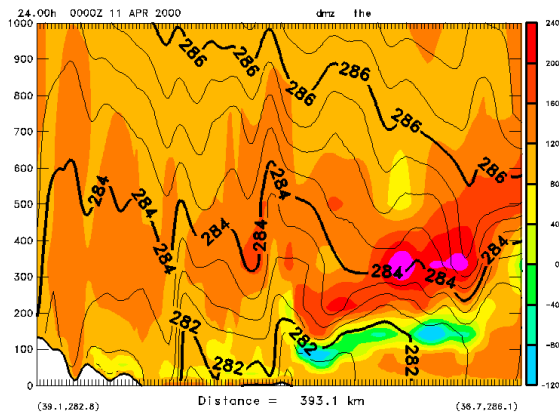


Fig. 3 Cross section of DM/Dz and isentropes of potential temperature (K) from surface to 1 km along line in Fig. 2b, at same time.

The vertical gradient of modified refractivity is displayed in Fig. 3. Discussion of modified refractivity,  $M$ , and its utility in defining expected propagation characteristics (e.g., ducting, super-refraction, sub-refraction, etc.) may be found in standard radar meteorology texts (Battan, 1973). Layers where  $DM/Dz$  is negative will tend to trap EM rays launched at a low elevation angle. Conversely, layers in which  $DM/Dz$  is strongly positive are subrefractive;

that is, the EM rays initially launched parallel with the Earth's surface will tend to bend away from the Earth with distance. Subrefraction occurs when  $DN/Dz \geq 0$ , where  $N$  is ordinary refractivity. This criterion is equivalent to  $DM/Dz \geq 157$  M-units/km.

Although admittedly difficult to see in the black-and-white version, Fig. 3 shows a trapping layer to be present over the Atlantic at the top of the well-mixed BL. Interestingly, in the strongly stratified region above the BL, a layer of subrefraction overlies the superrefractive layer. This appears to be due to differential moisture advection aloft and its impact upon the vertical moisture gradient. The superrefractive layer is associated with the typical sharp temperature and moisture gradients at the marine BL top. Gradients in atmospheric stratification across the several coastline boundaries of this cross section are seen to be closely correlated with changes in the  $DM/Dz$  field. The Tidewater Peninsula (just left of center in Fig. 3) is cool relative to its surroundings; local time is 1900 and the land has cooled below the surrounding SST.

While Fig. 3 shows what is happening along a particular cross section, Fig. 4 displays the isosurface of  $DM/Dz = 0$ , as viewed from above. That is, the

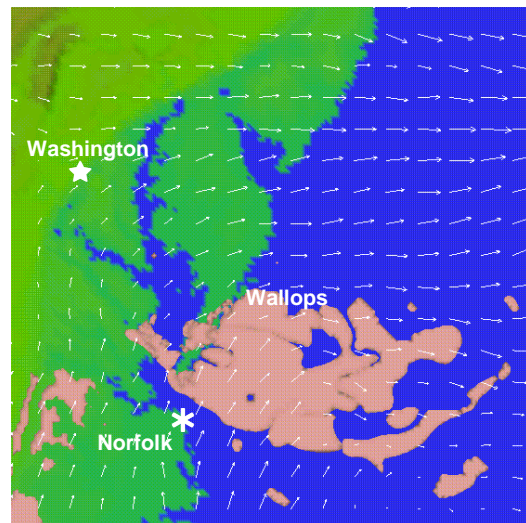


Fig. 4 COAMPS forecast trapping layer and 10-m wind vectors.

horizontal coverage of the trapping layer is shown by the irregular surface (primarily over the Atlantic) in Fig. 4. The trapping layer

resides at the northern end of the southerly BL flow. There is no trapping on the north side of the front where strong westerly flow is evident just north of Wallops in Fig. 4. Further exploration of the BL evolution producing this isolated region of elevated trapping is required.

Finally, Fig. 5 displays the EDH field (shaded and contoured). The EDH is computed as a diagnostic output parameter from COAMPS fields of SST, near surface wind, temperature, moisture, and surface pressure. At each COAMPS over water grid point, similarity profiles of T and Q (with M then derived from these quantities) are computed on a special grid having 1m vertical spacing from the surface to 40 m. The height of the minimum in M is then located on this grid and designated the EDH. This technique is further described in Cook and Burk (1992).



Fig. 5 Evaporation Duct Height (EDH) (m) on the 3 km COAMPS grid at 00 UTC 11 Apr 2000.

Figure 5 shows that, at least at this time, most of the gradient in EDH is along the coastlines rather than perpendicular to them. The southerly flow at this time crossing the spatially varying SST field likely

plays a large role in determining this EDH structure. Further study of the time period and comparison with the Wallops data set is ongoing.

#### ACKNOWLEDGEMENTS

Data from Wallops-2000 was kindly supplied to us by Dr. Rob Marshall of NSWCCD, Dr. Ken Davidson of the Naval Postgraduate School, and Dr. Ross Rottier of Johns Hopkins Univ. APL. This support of the sponsor, the Office of Naval Research, through program element 0602435N is gratefully acknowledged.

#### References

- Battan, L.J., 1973: *Radar Observations of the Atmosphere*. Univ. of Chi. Press, 324pp.
- Burk, S.D., T. Haack, L.T. Rogers, and L.J. Wagner, 2003 : Island wake dynamics and wake influence on the evaporation duct and radar propagation. *J. Appl. Meteor.*, **42**, 349-367.
- Cook, J., and S.D. Burk, 1992 : Potential refractivity as a similarity variable. *Bound.-Layer Meteor.*, **58**, 151-159.
- Haack, T. and S.D. Burk, 2001 : Summertime marine refractivity conditions along coastal California. *J. Appl. Meteor.*, **40**, 673-687.
- Hodur, R.M., J. Pullen, J. Cummings, X. Hong, J.D. Doyle, P. Martin, and M.A. Rennick, 2002 : The coupled ocean/atmosphere mesoscale prediction system (COAMPS). *Oceanography*, **15**, 88-89.
- Rogers, L.T., 1997 : Likelihood estimation of tropospheric duct parameters from horizontal propagation measurements. *Radio Sci.*, **32**, 79-92.

Corresponding author : Stephen D. Burk,  
Naval Research Laboratory, Marine  
Meteorology Division, 7 Grace Hopper Ave.,  
Monterey, CA 93943-5502:  
[burk@nrlmry.navy.mil](mailto:burk@nrlmry.navy.mil)